PROCEEDINGS OF THE ROYAL SOCIETY A | MATHEMATICAL, PHYSICAL & ENGINEERING SCIENCES

Reflection and refraction of antiplane shear waves at a plane boundary between viscoelastic anisotropic media

The Royal Society

Email alerting service	Receive free email alerts when new articles cite this article - sign up in the box at the top right-hand corner of the article or click **here**

Reflection and refraction of antiplane shear waves at a plane boundary between viscoelastic anisotropic media

By J. M. Carcione

Osservatorio Geofisico Sperimentale,
P.O. Box 2011 Opicina, 34016 Trieste, Italy

We consider two monoclinic viscoelastic media in contact, with the incidence and refraction planes coincident with the respective planes of symmetry. Then, an incident homogeneous antiplane shear wave generates pure reflected and refracted antiplane waves, whose slowness and Umov–Poynting vectors lie in the planes of symmetry. The simplicity of the problem permits a detailed investigation of the phenomena caused by the combined anisotropic–anelastic properties of the media and waves. A general approach and the analysis of a numerical example provide a complete picture of the physics. In general, the reflected and refracted waves are inhomogeneous, i.e. equiphase planes do not coincide with equiamplitude planes. The reflected wave is homogeneous only when the incidence medium is transversely isotropic, i.e. its symmetry axis is perpendicular to the interface. If the refraction medium is elastic, the refracted wave is inhomogeneous of the elastic type, i.e. the attenuation vector is perpendicular to the Umov–Poynting vector (energy direction). The angle between the attenuation and the real slowness vectors may exceed 90°, but the angle between the attenuation and the Umov–Poynting vector is always less than 90°. If the incidence medium is elastic, the attenuation of the refracted wave is perpendicular to the interface. As in the anisotropic elastic case, energy flow parallel to the interface is the criterion for obtaining a critical angle. As in the isotropic viscoelastic case, critical angles exist only in rare instances. Indeed, they do not exist if one of the media is elastic. The existence of Brewster angles (related to a zero reflection coefficient) is also severely restricted by anelasticity.

To balance the energy flux at the boundary, it is necessary to consider the interference flux between the incident and reflected waves (this flux vanishes in the elastic case). For the particular example, the refracted flux is always greater than zero and there is transmission for all the incident angles. This phenomenon is related to the absence of critical angles. For a transversely isotropic incidence medium, attenuations, quality factors and phase and energy velocities of the incident and reflected waves coincide for all the incidence angles.

It is important to point out that the relevant physical phenomena are related to the energy flow direction (Umov–Poynting vector) rather than to the propagation direction (real slowness vector). For instance, the characteristics of the elastic type inhomogeneous waves, the existence of critical angles, and the fact that the amplitudes of the reflected and refracted waves decay in the direction of energy flow despite the fact that they grow in the direction of phase propagation.

920   *J. M. Carcione*

1. Introduction

The antiplane shear problem is one of relative mathematical simplicity and includes the essential physics common to more complicated cases, where multiple and coupled deformations occur (Horgan 1995). In this sense, analysis of the reflection and refraction of antiplane shear waves may serve as a pilot problem for investigating the influence of anisotropy and/or anelasticity on solution behaviour.

As is well known, propagation in the plane of mirror symmetry of a monoclinic medium is the most general situation for which antiplane strain motion exists in all directions (the corresponding waves are also termed type-II S and SH in the geophysical literature (Borcherdt 1977; Helbig 1994)).

Besides the work by Hayes & Rivlin (1974), who considered a low-loss approximation, the study of wave propagation in anisotropic viscoelastic media is a relatively recent topic. Carcione & Cavallini (1993) and Romeo (1994) obtained some general relations that restrict the propagation of inhomogeneous waves. Concerning antiplane motion, Carcione (1994) studied the propagation of homogeneous plane waves in the plane of mirror symmetry of a viscoelastic transversely isotropic medium. Krebes & Le (1994) and Carcione & Cavallini (1995a) analysed the more general problem of inhomogeneous viscoelastic waves, that revealed the existence of forbidden propagation directions. Transient analytical solutions were obtained by Le (1993) and Carcione & Cavallini (1994), who also developed numerical simulation algorithms (Le *et al.* 1994; Carcione & Cavallini 1995b). Moreover, a confrontation between the plane wave theory and the transient solution is given in Carcione *et al.* (1996).

In the following, we consider two monoclinic media with a common mirror plane of symmetry in contact along a plane perpendicular to the symmetry plane. The incidence and refraction plane is taken to be coincident with this plane of symmetry. Then, an incident antiplane shear wave will generate reflected and refracted shear waves without conversion to the coupled quasi-compressional and quasi-shear modes.

The physics of the problem may differ depending on the values of the elastic constants and the anisotropic dissipation of the upper and lower media. For this reason, we follow a general treatment and, simultaneously, consider a numerical example including the essential physical aspects. In this way, the analysis provides further insight into the nature of the reflection–refraction problem.

2. Propagation in a homogeneous monoclinic medium

Assume a homogeneous viscoelastic monoclinic medium with the vertical (x_1, x_3)-plane as its single mirror symmetry plane. Then, antiplane shear waves with particle velocity $\boldsymbol{v} = v(x_1, x_3)\hat{\boldsymbol{e}}_2$ propagate, such that

$$v = \mathrm{i}\omega u_0 \exp[\mathrm{i}\omega(t - s_1 x_1 - s_3 x_3)], \tag{2.1}$$

where s_1 and s_3 are the components of the complex slowness vector, ω is the angular frequency satisfying $\omega \geqslant 0$, t is the time variable, u_0 is a complex quantity and $\mathrm{i} = \sqrt{-1}$. The real slowness and attenuation vectors are given by

$$\boldsymbol{s}_R = [\mathrm{Re}(s_1), \mathrm{Re}(s_3)]^\top, \tag{2.2}$$

and

$$\boldsymbol{\alpha} = -\omega[\mathrm{Im}(s_1), \mathrm{Im}(s_3)]^\top, \tag{2.3}$$

respectively, such that the complex slowness vector is $\boldsymbol{s} = \boldsymbol{s}_R - \mathrm{i}(\boldsymbol{\alpha}/\omega)$ (the symbol $\top$ denotes transpose).

The antiplane assumption implies that the only non-zero components of stress are σ_{12} and σ_{32} that satisfy the constitutive equations (Carcione & Cavallini 1995a)

$$i\omega\sigma_{12} = p_{46}\partial_3 v + p_{66}\partial_1 v \quad \text{and} \quad i\omega\sigma_{32} = p_{44}\partial_3 v + p_{46}\partial_1 v, \tag{2.4}$$

where p_{IJ} are the complex stiffnesses, and ∂_1 and ∂_3 denote spatial derivatives. As shown in §3, the p_{IJ} equal the real high-frequency limit c_{IJ} in the elastic case.

The complex slowness relation has the following simple form (Carcione 1994):

$$F(s_1, s_3) \equiv p_{44}s_3^2 + p_{66}s_1^2 + 2p_{46}s_1 s_3 - \rho = 0, \tag{2.5}$$

where ρ is the material density.

Let us assume that the positive x_3-axis points downwards. In order to distinguish between down and up propagating waves, the slowness relation is solved for s_3, given the horizontal slowness s_1. It yields

$$s_{3\pm} = \frac{1}{p_{44}} \left[-p_{46}s_1 \pm \text{PV}(\rho p_{44} - p^2 s_1^2)^{1/2} \right], \tag{2.6}$$

where

$$p^2 = p_{44}p_{66} - p_{46}^2 \tag{2.7}$$

and $\text{PV}(z)^{1/2}$ denotes the principal value of the square root of the complex number z. In principle, the $+$ sign corresponds to downward or $+x_3$ propagating waves, while the $-$ sign to upward or $-x_3$ propagating waves.

We recall that the group velocity equals the energy velocity only when there is no attenuation. Therefore, analysis of the physics requires explicit calculation of the energy velocity, since the concept of group velocity looses its physical meaning in anelastic media (Oughstun & Sherman 1994; Carcione 1994). The mean energy flux or time average Umov–Poynting vector $\langle\boldsymbol{P}\rangle$ is the real part of the corresponding complex vector (Auld 1990; Carcione & Cavallini 1993)

$$\boldsymbol{P} = -\tfrac{1}{2}(\sigma_{12}\hat{\boldsymbol{e}}_1 + \sigma_{32}\hat{\boldsymbol{e}}_3)v^*, \tag{2.8}$$

where the superscipt $*$ denotes complex conjugate. Substituting the plane wave (2.1) and the constitutive equations (2.4) into equation (2.8) gives

$$\boldsymbol{P} = \tfrac{1}{2}\omega^2|u_0|^2 \exp\{2\omega[\text{Im}(s_1)x_1 + \text{Im}(s_3)x_3]\}(X\hat{\boldsymbol{e}}_1 + Z\hat{\boldsymbol{e}}_3), \tag{2.9}$$

where

$$X = p_{66}s_1 + p_{46}s_3 \quad \text{and} \quad Z = p_{46}s_1 + p_{44}s_3. \tag{2.10}$$

For time harmonic fields, the time-average potential and dissipated energy densities, $\langle\epsilon_s\rangle$ and $\langle\epsilon_d\rangle$, can be obtained from a complex strain energy density (Carcione & Cavallini 1993), which for SH waves propagating in a monoclinic medium is given by

$$\Phi = \frac{1}{2}\text{Re}\left\{ p_{44}\left|\frac{\partial_3 v}{i\omega}\right|^2 + p_{66}\left|\frac{\partial_1 v}{i\omega}\right|^2 + 2p_{46}\text{Re}\left[\frac{\partial_3 v}{i\omega}\left(\frac{\partial_1 v}{i\omega}\right)^*\right] \right\}. \tag{2.11}$$

Then,

$$\langle\epsilon_s\rangle = \tfrac{1}{2}\text{Re}(\Phi), \quad \langle\epsilon_d\rangle = \text{Im}(\Phi) \tag{2.12}$$

(Carcione & Cavallini 1995a). Substituting the plane wave (2.1) into (2.11), the energy densities become

$$\langle\epsilon_s\rangle = \tfrac{1}{4}\omega^2|u_0|^2 \exp\{2\omega[\text{Im}(s_1)x_1 + \text{Im}(s_3)x_3]\}\text{Re}(\beta) \tag{2.13}$$

922   J. M. Carcione

and

$$\langle \epsilon_d \rangle = \tfrac{1}{2}\omega^2 |u_0|^2 \exp\{2\omega[\text{Im}(s_1)x_1 + \text{Im}(s_3)x_3]\}\text{Im}(\beta), \tag{2.14}$$

where

$$\beta = p_{44}|s_3|^2 + p_{66}|s_1|^2 + 2p_{46}\,\text{Re}(s_1^* s_3). \tag{2.15}$$

On the other hand, the time-average kinetic energy density is simply

$$\langle \epsilon_v \rangle = \tfrac{1}{4}\rho|v^2| = \tfrac{1}{4}\rho\omega^2|u_0|^2 \exp\{2\omega[\text{Im}(s_1)x_1 + \text{Im}(s_3)x_3]\}. \tag{2.16}$$

3. Complex stiffnesses of the incidence and refraction media: a numerical example

A realistic viscoelastic model is the standard linear solid, also called the Zener model (Zener 1948). It satisfies causality and gives relaxation and creep functions in agreement with experimental results (e.g. aluminium (Zener 1948) and shale (Johnston 1982)).

The present theory assigns different Zener elements to p_{44} and p_{66} in order to define the attenuation (or quality factor) along the horizontal and vertical directions (x_1 and x_3 axes), respectively. Hence, the stiffnesses are

$$p_{44} = c_{44}M_1, \quad p_{66} = c_{66}M_2, \quad p_{46} = c_{46}, \tag{3.1}$$

where

$$M_\nu = \frac{\tau_{\sigma\nu}}{\tau_{\epsilon\nu}}\left(\frac{1 + \mathrm{i}\omega\tau_{\epsilon\nu}}{1 + \mathrm{i}\omega\tau_{\sigma\nu}}\right), \quad \nu = 1, 2 \tag{3.2}$$

are the complex moduli (Ben-Menahem & Singh 1981). The relaxation times are given by

$$\tau_{\epsilon\nu} = \frac{\tau_0}{Q_{0\nu}}[\sqrt{Q_{0\nu}^2 + 1} + 1] \tag{3.3}$$

and

$$\tau_{\sigma\nu} = \frac{\tau_0}{Q_{0\nu}}[\sqrt{Q_{0\nu}^2 + 1} - 1], \tag{3.4}$$

where τ_0 is a characteristic relaxation time and $Q_{0\nu}$ is a characteristic quality factor. It can be shown that (see Carcione (1994) and §9) the quality factors for homogeneous waves along the axes are

$$Q_\nu = Q_{0\nu}\frac{1 + \omega^2\tau_0^2}{2\omega\tau_0}. \tag{3.5}$$

Then, $1/\tau_0$ is the angular frequency where the quality factor has the minimum value $Q_{0\nu}$. The choice $\tau_0 = \sqrt{\tau_{\epsilon 1}\tau_{\sigma 1}} = \sqrt{\tau_{\epsilon 2}\tau_{\sigma 2}}$ implies that the maximum dissipation for both mechanisms occurs at the same frequency. As $\omega \to \infty$, $M_\nu \to 1$ and the complex stiffnesses p_{IJ} approach the unrelaxed elastic constants c_{IJ}.

In the reflection–refraction problem, the upper medium is defined by the properties c_{IJ}, $Q_{0\nu}$ and τ_0, and the lower medium is defined by the corresponding primed quantities c'_{IJ}, $Q'_{0\nu}$ and τ'_0. The numerical example assumes that

$$c_{44} = 9.68\,\text{GPa}, \quad Q_{01} = 10, \tag{3.6}$$

$$c_{66} = 12.5\,\text{GPa}, \quad Q_{02} = 20, \tag{3.7}$$

and

$$c'_{44} = 19.6 \text{ GPa}, \quad Q'_{01} = 20, \tag{3.8}$$

$$c'_{66} = 25.6 \text{ GPa}, \quad Q'_{02} = 30. \tag{3.9}$$

Moreover,

$$c_{46} = -\tfrac{1}{2}\sqrt{c_{44}c_{66}}, \quad c'_{46} = \tfrac{1}{2}\sqrt{c'_{44}c'_{66}}, \tag{3.10}$$

and

$$\rho = 2 \text{ g cm}^{-3}, \quad \rho' = 2.5 \text{ g cm}^{-3}. \tag{3.11}$$

The characteristic relaxation time is taken as $\tau_0 = \tau'_0 = (2\pi f_0)^{-1}$, i.e. the maximum attenuation occurs at a frequency f_0. The above parameters give horizontal and vertical (elastic or unrelaxed) phase velocities of 2500 m s^{-1} and 2200 m s^{-1}, respectively, for the upper medium, and 3200 m s^{-1} and 2800 m s^{-1}, for the lower medium.

Several subcases treated in the analysis make use of the following limiting situations:

$$\text{elastic:} \quad Q_{0\nu} = Q'_{0\nu} = \infty (\tau_{\epsilon\nu} = \tau_{\epsilon\nu}, \tau'_{\epsilon\nu} = \tau'_{\epsilon\nu}) \quad \text{or} \quad M_\nu = M'_\nu = 1, \tag{3.12}$$

$$\text{isotropic:} \quad p_{44} = p_{66} = \mu, \quad p'_{44} = p'_{66} = \mu', \quad p_{46} = p'_{46} = 0, \tag{3.13}$$

$$\text{transversely isotropic:} \quad p_{46} = p'_{46} = 0. \tag{3.14}$$

Note, however, that the condition $p_{46} = p'_{46} = 0$ does not necessarily mean that the media are transversely isotropic.

The analysis of the problem is carried out at the frequency f_0 and therefore its value is immaterial. Moreover, at a fixed frequency, the analysis does not depend on the viscoelastic model. However, comparisons with the elastic case require a proper constitutive equation that behaves elastically at the low- and high-frequency limits.

4. Reflection and refraction coefficients

Let us assume that the incident, reflected and refracted waves are identified by the superscripts I, R and T. The solution to the problem parallels that of the elastic case (Musgrave 1970; Auld 1990; Schoenberg & Costa 1991) with the difference that here the stiffnesses and slowness components are complex quantities.

The particle velocity of the incident wave can be written as

$$v^{\text{I}} = \mathrm{i}\omega \exp[\mathrm{i}\omega(t - s_1 x_1 - s_3^{\text{I}} x_3)], \tag{4.1}$$

where, for simplicity, the superscript I in the horizontal slowness has been omitted here and in all the subsequent analysis.

Inhomogeneous viscoelastic plane waves have the property that equiphase planes (normal to the real slowness vector) do not coincide with equiamplitude planes (normal to the attenuation vector). When the directions of propagation and attenuation coincide, the wave is called homogeneous. For a homogeneous wave (Carcione 1994),

$$s_1 = \sin\theta^{\text{I}}/V(\theta^{\text{I}}), \quad s_3^{\text{I}} = \cos\theta^{\text{I}}/V(\theta^{\text{I}}), \tag{4.2}$$

where θ^{I} is the incidence propagation (attenuation) angle (see figure 1), and

$$V(\theta) = [(p_{44}\cos^2\theta + p_{66}\sin^2\theta + p_{46}\sin 2\theta)/\rho]^{1/2} \tag{4.3}$$

is the complex velocity.

As in the isotropic–viscoelastic case (Buchen 1971; Schoenberg 1971; Borcherdt 1977; Caviglia & Morro 1992), the boundary conditions (continuity of v and σ_{32}) give the reflection and transmission coefficients. Snell's law, i.e. the continuity of the horizontal complex slowness:

$$s_1^{\mathrm{R}} = s_1^{\mathrm{T}} = s_1, \tag{4.4}$$

is a necessary condition for the existence of the boundary conditions.

Denoting the reflection and refraction coefficients by R and T, the particle velocities of the reflected and refracted waves are given by

$$v^{\mathrm{R}} = \mathrm{i}\omega R \exp[\mathrm{i}\omega(t - s_1 x_1 - s_3^{\mathrm{R}} x_3)] \tag{4.5}$$

and

$$v^{\mathrm{T}} = \mathrm{i}\omega T \exp[\mathrm{i}\omega(t - s_1 x_1 - s_3^{\mathrm{T}} x_3)], \tag{4.6}$$

respectively.

Then, continuity of v and σ_{32} at $x_3 = 0$ gives

$$T = 1 + R \tag{4.7}$$

and

$$Z_{\mathrm{I}} + R Z_{\mathrm{T}} = T Z_{\mathrm{T}}, \tag{4.8}$$

which have the following solution:

$$R = \frac{Z^{\mathrm{I}} - Z^{\mathrm{T}}}{Z^{\mathrm{T}} - Z^{\mathrm{R}}}, \quad T = \frac{Z^{\mathrm{I}} - Z^{\mathrm{R}}}{Z^{\mathrm{T}} - Z^{\mathrm{R}}}. \tag{4.9}$$

Since both the incident and reflected waves satisfy the slowness relation (2.5), the vertical slowness s_3^{R} can be obtained by subtracting $F(s_1, s_3^{\mathrm{I}})$ from $F(s_1, s_3^{\mathrm{R}})$ and assuming $s_3^{\mathrm{R}} \neq s_3^{\mathrm{I}}$. It yields

$$s_3^{\mathrm{R}} = -\left(s_3^{\mathrm{I}} + \frac{2 p_{46}}{p_{44}} s_1\right). \tag{4.10}$$

Then, using equation (2.10) we obtain $Z^{\mathrm{R}} = -Z^{\mathrm{I}}$ and the reflection and transmission coefficients (4.9) become

$$R = \frac{Z^{\mathrm{I}} - Z^{\mathrm{T}}}{Z^{\mathrm{I}} + Z^{\mathrm{T}}}, \quad T = \frac{2 Z^{\mathrm{I}}}{Z^{\mathrm{I}} + Z^{\mathrm{T}}}, \tag{4.11}$$

in agreement with Schoenberg & Costa (1991).

The slowness relation (2.5) of the refraction medium gives s_3^{T} in terms of s_1:

$$s_3^{\mathrm{T}} = \frac{1}{p_{44}'}[-p_{46}' s_1 + \mathrm{PV}(\rho' p_{44}' - p'^2 s_1^2)^{1/2}], \tag{4.12}$$

with

$$p'^2 = p_{44}' p_{66}' - p_{46}'^2. \tag{4.13}$$

Alternatively, from equation (2.10),

$$s_3^{\mathrm{T}} = \frac{1}{p_{44}'}(Z^{\mathrm{T}} - p_{46}' s_1). \tag{4.14}$$

Figure 1 represents the incident (I), reflected (R) and transmitted (T) waves at a boundary between two linear viscoelastic and monoclinic media. The angles θ, δ and
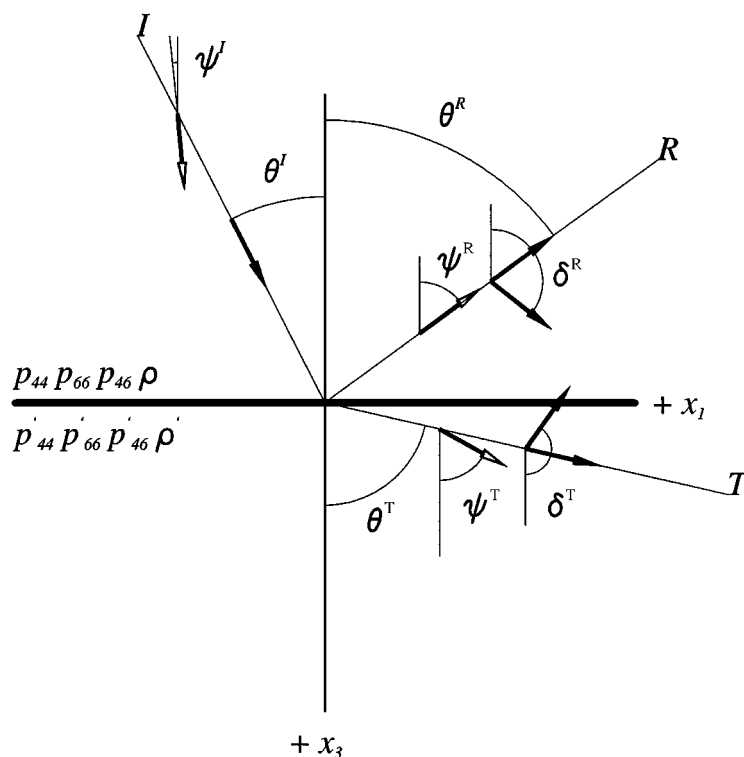
Figure 1. Incident (I), reflected (R) and transmitted (T) waves at a boundary between two linear viscoelastic and monoclinic media. The angles θ, δ and ψ denote the propagation, attenuation and Umov–Poynting vector (energy) directions. The reflection angle is negative as shown.

ψ denote the propagation, attenuation and Umov–Poynting vector (energy) directions. Note that the propagation and energy directions do not necessarily coincide. Moreover, $|\theta - \delta|$ may exceed $90°$ in anisotropic viscoelastic media (Krebes & Le 1994; Carcione & Cavallini 1995a), while $|\theta - \delta|$ is strictly less than $90°$ in isotropic media (Borcherdt 1977).

5. Propagation, attenuation and energy directions

The fan of incident rays is determined by the condition that the energy propagation direction is downwards $(+x_3)$ and to the right $(+x_1)$. The limiting rays for the numerical example are represented in figures 2a $(\theta^I = 24.76°)$ and 2b $(\theta^I = 58.15°)$ $(23.75°$ and $60.39°$, respectively, in the elastic case). The larger curve is the slowness for homogeneous waves in the incidence medium, and the other curve is the slowness for homogeneous waves in the refraction medium (Carcione 1994). In general, the energy direction of each ray is not perpendicular to the corresponding slowness curve. The orthogonality property is only verified in the elastic case (Carcione 1994).

Given the components of the complex slowness vector, the propagation and attenuation angles θ and δ for all the waves are

$$\tan(\theta) = \frac{\mathrm{Re}(s_1)}{\mathrm{Re}(s_3)} \tag{5.1}$$

J. M. Carcione
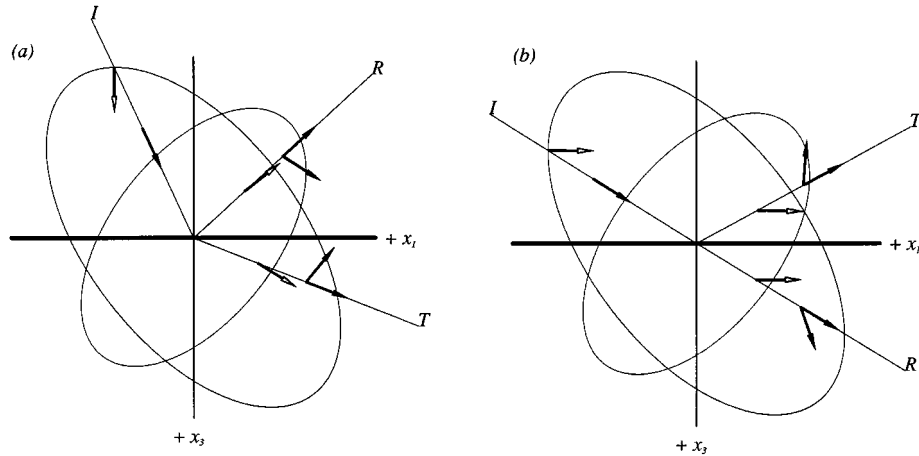
Figure 2. Limiting rays for the fan of incident angles. (a) $\theta^{\mathrm{I}} = 24.76°$ and (b) $\theta^{\mathrm{I}} = 58.15°$ ($23.75°$ and $60.39°$, respectively, in the elastic case). They are determined by the condition that the energy propagation direction is downwards ($+x_3$) and to the right ($+x_1$), i.e. $0 \leqslant \psi^{\mathrm{I}} \leqslant 90°$. The larger curve is the slowness for homogeneous waves in the incidence medium and the other curve is the slowness for homogeneous waves in the refraction medium.

and

$$\tan(\delta) = \frac{\mathrm{Im}(s_1)}{\mathrm{Im}(s_3)}. \tag{5.2}$$

These equations can be easily verified for the incident wave (4.1), for which $\delta^{\mathrm{I}} = \theta^{\mathrm{I}}$, by virtue of equation (4.2).

Moreover, from equations (4.5) and (4.10), the reflection, propagation and attenuation angles are

$$\tan(\theta^{\mathrm{R}}) = -\frac{\mathrm{Re}(s_1)}{\mathrm{Re}(s_3^{\mathrm{I}} + 2p_{46}p_{44}^{-1}s_1)} \tag{5.3}$$

and

$$\tan(\delta^{\mathrm{R}}) = -\frac{\mathrm{Im}(s_1)}{\mathrm{Im}(s_3^{\mathrm{I}} + 2p_{46}p_{44}^{-1}s_1)}, \tag{5.4}$$

respectively. Unlike the isotropic case (Borcherdt 1977), the reflected wave is, in general, inhomogeneous.

Theorem 5.1. *If the incident wave is homogeneous and not normally incident, the reflected wave is homogeneous if and only if* $\mathrm{Im}(p_{46}/p_{44}) = 0$.

Proof. Assume that the reflected wave is homogeneous. Then, $\tan\theta^{\mathrm{R}} = \tan\delta^{\mathrm{R}}$ implies that $\mathrm{Im}[s_1^*(s_3^{\mathrm{I}} + 2p_{46}p_{44}^{-1}s_1)] = 0$. Assuming $\theta^{\mathrm{I}} \neq 0$ and using equation (4.2) gives $\mathrm{Im}(p_{46}/p_{44}) = 0$. The same reasoning shows that this constraint implies a homogeneous reflected wave. ∎

An immediate corollary of theorem 5.1 is as follows.

Corollary 5.2. *If the upper medium has* $p_{46} = 0$, *the reflected wave is homogeneous. This follows immediately from theorem 5.1.*

In the elastic case, all the quantities in equation (5.3) are real, and the incidence

and reflection angles are related by

$$\cot(\theta^{\mathrm{R}}) = -\left(\cot\theta^{\mathrm{I}} + 2\frac{c_{46}}{c_{44}}\right). \tag{5.5}$$

From equation (4.6), the refraction propagation and attenuation angles are

$$\tan(\theta^{\mathrm{T}}) = \frac{\mathrm{Re}(s_1)}{\mathrm{Re}(s_3^{\mathrm{T}})} \tag{5.6}$$

and

$$\tan(\delta^{\mathrm{T}}) = \frac{\mathrm{Im}(s_1)}{\mathrm{Im}(s_3^{\mathrm{T}})}, \tag{5.7}$$

respectively. In general, the refracted wave is inhomogeneous.

Theorem 5.3. *If the refraction medium is elastic, the refracted wave is inhomogeneous of the elastic type; that is, the attenuation and Umov–Poynting vectors are perpendicular, i.e. $|\psi^{\mathrm{T}} - \delta^{\mathrm{T}}| = 90°$.*

Proof. The dissipated energy density for antiplane inhomogeneous waves in the plane of symmetry of a monoclinic medium was calculated by Krebes & Le (1994) and Carcione & Cavallini (1995a). For the refracted wave it is

$$\langle\epsilon_d^{\mathrm{T}}\rangle = \tfrac{1}{2}|T|^2 \exp\{2\omega[\mathrm{Im}(s_1)x_1 + \mathrm{Im}(s_3^{\mathrm{T}})x_3]\}\mathrm{Im}(\beta^{\mathrm{T}}), \tag{5.8}$$

where

$$\beta^{\mathrm{T}} = p_{44}'|s_3^{\mathrm{T}}|^2 + p_{66}'|s_1|^2 + 2p_{46}'\,\mathrm{Re}(s_1^*s_3^{\mathrm{T}}). \tag{5.9}$$

Since the medium is elastic ($p_{IJ}' \to c_{IJ}'$), β^{T} is real and $\langle\epsilon_d^{\mathrm{T}}\rangle = 0$. On the other hand, Carcione & Cavallini (1993) showed that an inhomogeneous wave propagating in a general three-dimensional anisotropic viscoelastic medium satisfies

$$\langle\epsilon_d^{\mathrm{T}}\rangle = \frac{2}{\omega}\boldsymbol{\alpha}^{\mathrm{T}\top} \cdot \langle\boldsymbol{P}^{\mathrm{T}}\rangle, \tag{5.10}$$

where the dot indicates the ordinary matrix product. Since the energy loss is zero, it is clear from equation (5.10) that $\boldsymbol{\alpha}^{\mathrm{T}}$ is perpendicular to the average Umov–Poynting vector $\langle\boldsymbol{P}^{\mathrm{T}}\rangle$. ∎

The existence of an inhomogeneous elastic plane wave propagating away from the interface is not intuitively obvious, since it is not the usual interface wave with attenuation vector perpendicular to the boundary. Elastic inhomogeneous body waves appear, for instance, in the expansion of a spherical wave (Brekhovskikh 1960).

Corollary 5.4. *Theorem 5.3 implies that, in general, the attenuation direction of the elastic refracted wave is not perpendicular to the propagation direction. That is, $\boldsymbol{\alpha}^{\mathrm{T}\top} \cdot \boldsymbol{s}_R^{\mathrm{T}} \neq 0$, or*

$$\mathrm{Re}(s_1)\mathrm{Im}(s_1) + \mathrm{Re}(s_3^{\mathrm{T}})\mathrm{Im}(s_3^{\mathrm{T}}) \neq 0. \tag{5.11}$$

In fact, the orthogonality property only happens in the isotropic case (Romeo 1994). Assume for simplicity transverse isotropy. Perpendicularity implies that $\mathrm{Im}(s_1^2 + s_3^{\mathrm{T}2}) = 0$, and using the slowness relation (2.5) we obtain

$$\mathrm{Im}(s_1^2)(c_{66}' - c_{44}') = 0, \tag{5.12}$$

which gives $c_{66}' = c_{44}'$ (i.e. isotropy).

Proposition 5.5. *If the incidence medium is elastic, the attenuation of the refracted wave is perpendicular to the interface.*

This result follows immediately from equation (5.7), since s_1 real (see equation (4.2)) implies $\delta^{\mathrm{T}} = 0$.

The expressions of the time average reflected and refracted Umov–Poynting vectors are obtained from equation (2.9), with $u_0 = R$ and $u_0 = T$, respectively. Then, the propagation angles of the incident, reflected and refracted energy vectors are obtained from

$$\tan \psi^{\mathrm{I}} = \frac{\mathrm{Re}(X^{\mathrm{I}})}{\mathrm{Re}(Z^{\mathrm{I}})}, \tag{5.13}$$

$$\tan \psi^{\mathrm{R}} = \frac{\mathrm{Re}(X^{\mathrm{R}})}{\mathrm{Re}(Z^{\mathrm{R}})} \tag{5.14}$$

and

$$\tan \psi^{\mathrm{T}} = \frac{\mathrm{Re}(X^{\mathrm{T}})}{\mathrm{Re}(Z^{\mathrm{T}})}, \tag{5.15}$$

respectively. Since from equations (2.10) and (4.10) $Z^{\mathrm{R}} = -Z^{\mathrm{I}}$ and $X^{\mathrm{R}} = X^{\mathrm{I}} - 2p_{46}p_{44}^{-1}Z^{\mathrm{I}}$, then

$$\tan \psi^{\mathrm{R}} = \frac{2\,\mathrm{Re}(p_{46}p_{44}^{-1}Z^{\mathrm{I}})}{\mathrm{Re}(Z^{\mathrm{I}})} - \tan \psi^{\mathrm{I}}. \tag{5.16}$$

In the elastic case,

$$\tan \psi^{\mathrm{R}} = 2c_{46}c_{44}^{-1} - \tan \psi^{\mathrm{I}}. \tag{5.17}$$

In the evaluation of each angle, particular attention should be given to the choice of the branch of the arctangent.

Figure 3 represents the propagation, attenuation and energy angles for the fan of incident rays. Note that the energy angle of the incident wave satisfies $0° \leqslant \psi^{\mathrm{I}} \leqslant 90°$ and that the inhomogeneity angles of the reflected and refracted waves ($|\theta^{\mathrm{R}} - \delta^{\mathrm{R}}|$ and $|\theta^{\mathrm{T}} - \delta^{\mathrm{T}}|$, respectively) never exceed 90°. However, consider a refraction medium with stronger dissipation; for instance, $Q'_{01} = 2$ and $Q'_{02} = 3$. In this case, $|\theta^{\mathrm{T}} - \delta^{\mathrm{T}}| > 90°$ for $\theta^{\mathrm{I}} \geqslant 50.46°$, meaning that the amplitude of the refracted wave grows in the direction of phase propagation. A physical interpretation of this phenomenon was given by Krebes & Le (1994) who showed that the amplitude of an inhomogeneous wave decays in the direction of energy propagation, i.e. in our case, $|\psi^{\mathrm{T}} - \delta^{\mathrm{T}}|$ is always less than 90°. Indeed, since the energy loss is always positive (Krebes & Le 1994; Carcione & Cavallini 1995*a*), equation (5.10) implies that the magnitude of the angle between $\boldsymbol{\alpha}^{\mathrm{T}}$ and $\langle \boldsymbol{P}^{\mathrm{T}} \rangle$ is always strictly less than 90°.

Proposition 5.6. *There is an incidence angle θ_0^{I} such that the incident and reflected propagation directions coincide, i.e. $\theta_0^{\mathrm{I}} - \theta^{\mathrm{R}} = 180°$. Moreover, the corresponding incident Umov–Poynting vector is parallel to the boundary.*

The angle can be found by equating (5.1) with (5.3) and using equation (2.10). It yields

$$\mathrm{Re}(Z^{\mathrm{I}}) = 0, \tag{5.18}$$

whose solution is $\theta_0^{\mathrm{I}} = 58.15°$, which corresponds to figure 2*b*. In the elastic case, we obtain

$$\theta_0^{\mathrm{I}} = -\arctan(c_{44}/c_{46}), \tag{5.19}$$
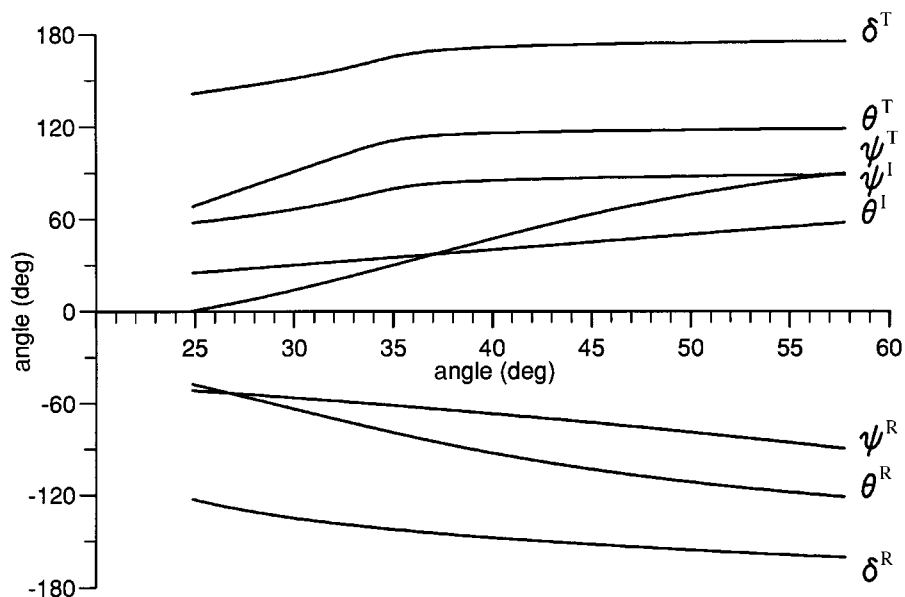
Figure 3. Propagation, attenuation and energy angles for the incident, reflected and refracted waves versus the incidence angle θ^{I}.

whose solution is $\theta_0^{\mathrm{I}} = 60.39°$. The angle is $90°$ in the isotropic case.

Proposition 5.7. *There is an incidence angle θ_1^{I} such that the reflected and refracted propagation directions coincide, i.e. $\theta^{\mathrm{T}} - \theta^{\mathrm{R}} = 180°$.*

The angle is obtained from equations (5.3) and (5.6) and the solution is $\theta_1^{\mathrm{I}} = 33.40°$, with $\theta^{\mathrm{R}} = -74.46°$. There is an explicit expression in the elastic case, that can be obtained from equations (4.2), (4.3), (4.12), (5.3) and (5.6). It gives

$$\tan(\theta_1^{\mathrm{I}}) = (-b - \sqrt{b^2 - 4ac})/(2a), \tag{5.20}$$

where

$$a = \rho' c_{66} - \rho c_{66}' + 4\rho c_{46}(c_{46}' c_{44} - c_{46} c_{44}')/c_{44}^2, \tag{5.21}$$

$$b = 2(\rho' c_{46} + \rho c_{46}' - 2\rho c_{46} c_{44}'/c_{44}) \tag{5.22}$$

and

$$c = \rho' c_{44} - \rho c_{44}'. \tag{5.23}$$

The solution is $\theta_1^{\mathrm{I}} = 34.96°$ and $\theta^{\mathrm{R}} = -73.63°$. In the isotropic case, $a = c$, $b = 0$ and there is no solution.

This situation is shown in figure 4, where the Poynting and attenuation vectors of the reflected (refracted) wave point upward (downward) and downward (upward), respectively. Thus, there is no contradiction since the energy of the refracted wave is actually pointing to the lower medium.

Proposition 5.8. *There is an incidence angle θ_2^{I} such that the propagation direction of the incident wave coincides with the corresponding Umov–Poynting vector direction, i.e. $\theta^{\mathrm{I}} = \psi^{\mathrm{I}} = \theta_2^{\mathrm{I}}$. This angle is related to the symmetry axis of the incidence medium, which is a pure mode direction where the waves behave as in isotropic media.*
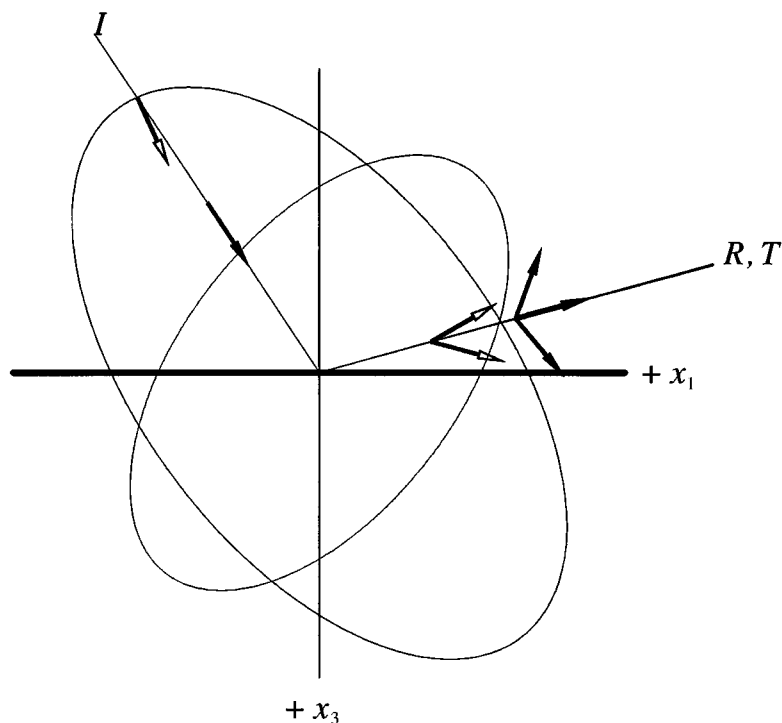
Figure 4. At the incidence angle $\theta_1^{\mathrm{I}} = 33.40°$ the reflected and refracted propagation directions coincide. However, note that the Poynting vector of the refracted wave (empty arrow) points downward.

From equations (5.1) and (5.13), this is verified when

$$\frac{\mathrm{Re}(s_1)}{\mathrm{Re}(s_3^{\mathrm{I}})} = \frac{\mathrm{Re}(X^{\mathrm{I}})}{\mathrm{Re}(Z^{\mathrm{I}})}. \tag{5.24}$$

Using equations (2.10) and (4.2) and after some algebra,

$$\tan(\theta_2^{\mathrm{I}}) = \{\mathrm{Re}(p_{66} - p_{44}) - [(\mathrm{Re}^2(p_{66} - p_{44}) + 4\,\mathrm{Re}^2(p_{46})]^{1/2}\}/[2\,\mathrm{Re}(p_{46})]. \tag{5.25}$$

The solution is $\theta_2^{\mathrm{I}} = 36.99°$. In the isotropic case, $\psi^{\mathrm{I}} = \theta^{\mathrm{I}}$ for all incident rays.

Proposition 5.9. *There is an incidence angle θ_3^{I} such that the propagation direction of the reflected wave coincides with the corresponding Umov–Poynting vector direction, i.e. $\theta^{\mathrm{R}} = \psi^{\mathrm{R}}$. From equations (5.3) and (5.14), this is verified when*

$$\frac{\mathrm{Re}(s_1)}{\mathrm{Re}(s_3^{\mathrm{R}})} = \frac{\mathrm{Re}(X^{\mathrm{R}})}{\mathrm{Re}(Z^{\mathrm{R}})}. \tag{5.26}$$

The solutions are $\theta_3^{\mathrm{I}} = 26.74°$ and $\theta^{\mathrm{R}} = -53.30°$. In the elastic case,

$$\tan(\theta_3^{\mathrm{I}}) = (-b - \sqrt{b^2 - 4ac})/(2a), \tag{5.27}$$

where

$$a = c_{46}\left(2\frac{d}{c_{44}^2} - 1\right), \quad b = \frac{c_{44}}{c_{46}}a - c_{66}, \quad c = -c_{46}, \tag{5.28}$$

with

$$d = c_{44}c_{66} - 2c_{46}^2. \tag{5.29}$$

The corresponding reflection angle is obtained from equations (5.3) and (5.14):

$$\tan(\theta_3^{\mathrm{R}}) = \{c_{66} - c_{44} + [(c_{66} - c_{44})^2 + 4c_{46}^2]^{1/2}\}/(2c_{46}). \tag{5.30}$$

The solutions are $\theta_3^{\mathrm{I}} = 27.61°$ and $\theta_3^{\mathrm{R}} = -52.19°$. In the elastic case, the reflection angle corresponds to the direction along the slowness ellipse. In the isotropic case $\psi^{\mathrm{R}} = \theta^{\mathrm{R}}$ for all incident rays.

Proposition 5.10. *An incident wave whose energy flux vector is parallel to the interface $[\mathrm{Re}(Z^{\mathrm{I}}) = 0]$ generates a reflected wave whose energy flux vector is parallel to the interface $[\mathrm{Re}(Z^{\mathrm{R}}) = 0]$. Moreover, in the elastic case and beyond the critical angle, the refracted energy flux vector is parallel to the interface $[\mathrm{Re}(Z^{\mathrm{T}}) = 0]$.*

Assuming $\mathrm{Re}(Z^{\mathrm{I}}) = 0$, and combining equations (2.10) and (4.10) gives $\mathrm{Re}(Z^{\mathrm{R}}) = 0$. On the other hand, from equations (4.12) and (4.14),

$$Z^{\mathrm{T}} = \mathrm{PV}(\rho' p'_{44} - p'^2 s_1^2)^{1/2}. \tag{5.31}$$

In the elastic limit of the example, a grazing incident wave generates a supercritical refracted wave. Beyond the critical angle, Z^{T} is purely imaginary (see §6), consequently $\mathrm{Re}(Z^{\mathrm{T}}) = 0$.

6. Brewster and critical angles

David Brewster in 1815 noted the existence of an angle (θ_{B}) such that: *if light is incident under this angle, the electric vector of the reflected light has no component in the plane of incidence* (Born & Wolf 1964). When this happens, $\theta_{\mathrm{B}} + \theta^{\mathrm{T}} = 90°$ and the reflection coefficient of the wave with electric vector in the plane of incidence vanishes. Here, we define the Brewster angle as the incidence angle for which $R = 0$ (note that in elastodynamics $\theta_{\mathrm{B}} + \theta^{\mathrm{T}} \neq 90°$ in general).

From equation (4.9), this occurs when $Z^{\mathrm{I}} = Z^{\mathrm{T}}$, or from (2.10), when

$$p_{46}s_1 + p_{44}s_3^{\mathrm{I}} = p'_{46}s_1 + p'_{44}s_3^{\mathrm{T}}. \tag{6.1}$$

Using (4.2), (4.3) and (4.12), equation (6.1) yields the following solution

$$\cot(\theta_{\mathrm{B}}) = (-b \pm \mathrm{PV}\sqrt{b^2 - 4ac})/(2a), \tag{6.2}$$

where

$$a = p_{44}(\rho p_{44} - \rho' p'_{44})/\rho, \quad b = 2p_{46}a/p_{44}, \tag{6.3}$$

and

$$c = p_{46}^2 - p'^{\,2}_{46} - p'_{44}(\rho' p_{66} - \rho p'_{66})/\rho. \tag{6.4}$$

In general, $\cot(\theta_{\mathrm{B}})$ is complex and there is no Brewster angle. In the elastic limit of the example the Brewster angle is $\theta_{\mathrm{B}} = 32.34°$ (see figure 5). In the isotropic viscoelastic case, the solution is

$$\cot(\theta_{\mathrm{B}}) = \pm \mathrm{PV} \left(\frac{\rho' - \rho\mu'/\mu}{\rho\mu/\mu' - \rho'} \right)^{1/2}, \tag{6.5}$$

which is, in general, complex for viscoelastic media. Actually, the Brewster angle exists only in rare instances. For example, $\cot(\theta_{\mathrm{B}})$ is real for $\mathrm{Im}(\mu/\mu') = 0$. Since the quality factor for homogeneous waves is $Q = \mathrm{Re}(\mu)/\mathrm{Im}(\mu)$ (Krebes 1983), the Brewster angle exists when $Q = Q'$, where $Q' = \mathrm{Re}(\mu')/\mathrm{Im}(\mu')$.

In anisotropic media, two singular angles can be defined depending on the orientation of the propagation and Umov–Poynting vectors with respect to the interface. The pseudocritical angle θ_P is defined as the angle of incidence for which the refracted real slowness vector is parallel to the interface. In Auld (1990), the critical angle phenomenon is related to the condition $s_3^T = 0$, but this is only valid when the lower medium has $p'_{46} = 0$ (e.g. transversely isotropic). The correct interpretation was given by Henneke II (1971), who defined the critical angle θ_C as the angle(s) of incidence beyond which the refracted Umov–Poynting vector is parallel to the interface (see also Rokhlin *et al.* (1986)). We keep the same interpretation for viscoelastic media. Actually, the pseudocritical angle does not play any important physical role in the anisotropic case. It can be shown that if $p_{46} = 0$, $\theta_C = \theta_P$.

The condition $\mathrm{Re}(Z^T)=0$ in equation (5.15) yields the critical angle θ_C. Using equation (2.10) this gives

$$\mathrm{Re}[p'_{46}s_1 + p'_{44}s_3^T] = 0, \tag{6.6}$$

or, from (4.12) and (4.14),

$$\mathrm{Re}[\mathrm{PV}(\rho'p'_{44} - p'^2 s_1^2)^{1/2}] = 0. \tag{6.7}$$

Since for a complex number z it is $[\mathrm{Re}(\sqrt{z})]^2 = \frac{1}{2}[|z| + \mathrm{Re}(z)]$, equation (6.7) is equivalent to

$$\mathrm{Im}(\rho'p'_{44} - p'^2 s_1^2) = 0, \quad \rho'p'_{44} - p'^2 s_1^2 \leqslant 0. \tag{6.8}$$

For the particular case when $\rho'p'_{44} - p'^2 s_1^2 = 0$, the following explicit solution is obtained

$$\cot(\theta_C) = \frac{1}{p_{44}}\left[-p_{46} + \mathrm{PV}\left(\frac{\rho p_{44}}{\rho'p'_{44}}p'^2 - p^2\right)^{1/2}\right]. \tag{6.9}$$

There is a solution if the right-hand side of equation (6.9) is real, which occurs only in very particular situations. However, the equation is general for the elastic case.

A critical angle exists in the isotropic case if

$$\cot^2(\theta_C) = \frac{\rho}{\rho'}\frac{\mu'}{\mu} - 1 \tag{6.10}$$

is a real quantity. This is verified for μ'/μ real or $Q = Q'$. Then, $\mu'/\mu = \mathrm{Re}(\mu')/\mathrm{Re}(\mu)$ and

$$\sin(\theta_P) = \left[\frac{\rho'\,\mathrm{Re}(\mu)}{\rho\,\mathrm{Re}(\mu')}\right]^{1/2}, \tag{6.11}$$

in agreement with Borcherdt (1977).

Figure 5 shows the absolute values of the reflection and transmission coefficients versus the incidence angle for the elastic (dotted line) and viscoelastic cases, respectively, with $\theta_P = 31.38°$, $\theta_B = 32.34°$ and $\theta_C = 36.44°$. The directions of real slowness and Umov–Poynting vectors, corresponding to the critical angle θ_C, can be appreciated in figure 6 (elastic case). At the critical angle and beyond, the refracted Umov–Poynting vector is parallel to the interface and the wave becomes evanescent. In fact, beyond the critical angle, the horizontal slowness s_1 is greater than $(\rho'c'_{44})^{1/2}/c'$, where $c' = c'_{44}c'_{66} - c'_{46}$ (Schoenberg & Costa 1991). Therefore, the quantity $\rho'c'_{44} - c'^2 s_1^2$ becomes negative, $\mathrm{Re}(Z^T) = 0$ and the vertical component of the refracted slowness vector s_3^T becomes complex (see equation (4.12)). A geometrical interpretation is that, in the elastic case, critical angles are associated with
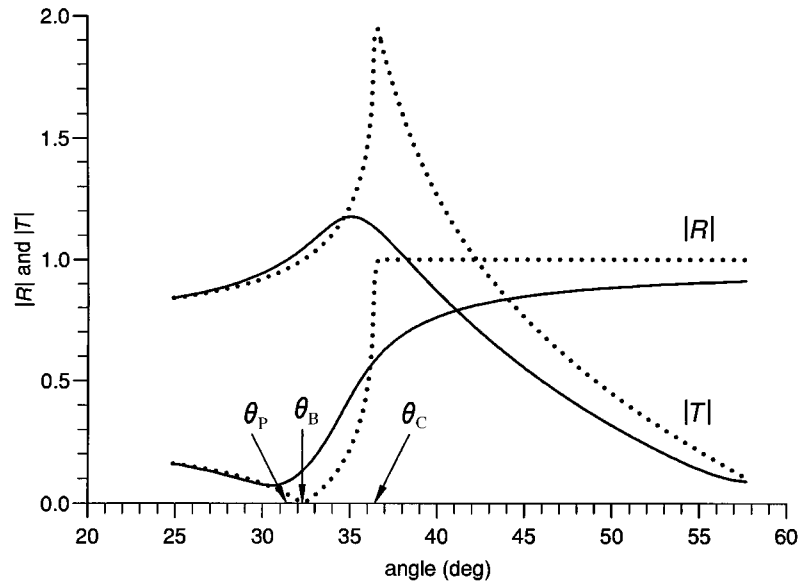
Figure 5. Absolute values of the reflection and transmission coefficients versus the incidence angle for the elastic (dotted line) and viscoelastic (continuous line) cases ($\theta_P = 31.38°$, $\theta_B = 32.34°$ and $\theta_C = 36.44°$).

tangent planes to the slowness surface that are normal to the interface (see figure 6). Snell's law requires that the end points of all the slowness vectors lie in a common normal line to the interface. We get the critical angle when this line is tangent to the slowness curve of the refraction medium. Beyond the critical angle there is no intersection between that line and the slowness curve, and the wave becomes evanescent (Henneke II 1971; Rokhlin *et al.* 1986; Helbig 1994).

According to proposition 5.10, the Umov–Poynting vector is parallel to the boundary beyond the critical angle. Moreover, since Z^T is purely imaginary, equations (4.12) and (5.31) imply that $\mathrm{Re}(s_3^T) = -c'_{46}s_1/c'_{44}$. Finally, using equation (5.6) we obtain the refracted propagation angle

$$\theta^T = -\arctan(c'_{44}/c'_{46}). \tag{6.12}$$

This angle takes the value $\theta^T = 119.75°$ ($\psi^T = 90°$) and remains constant for $\theta^I \geqslant \theta_C$. This phenomenon does not occur in the anelastic case.

As can be seen in figure 5, there is no critical angle in the viscoelastic case and the reflection coefficient is always greater than zero (no Brewster angle). As in the isotropic case (Borcherdt 1977), critical angles exist under very particular conditions.

Theorem 6.1. *If one of the media is elastic and the other is anelastic, then there are no critical angles.*

Proof. Suppose there exists a critical angle; that is, the refracted Umov–Poynting vector is parallel to the interface. Assume first that the incidence medium is elastic. Proposition 5.5 implies that the attenuation of the refracted wave is normal to the interface. However, since the refraction medium is anelastic, such an inhomogeneous (elastic) wave cannot propagate.

Conversely, assume non-normal incidence and that the refraction medium is elastic. Since the incidence medium is anelastic, Snell's law requires a transmitted inho-
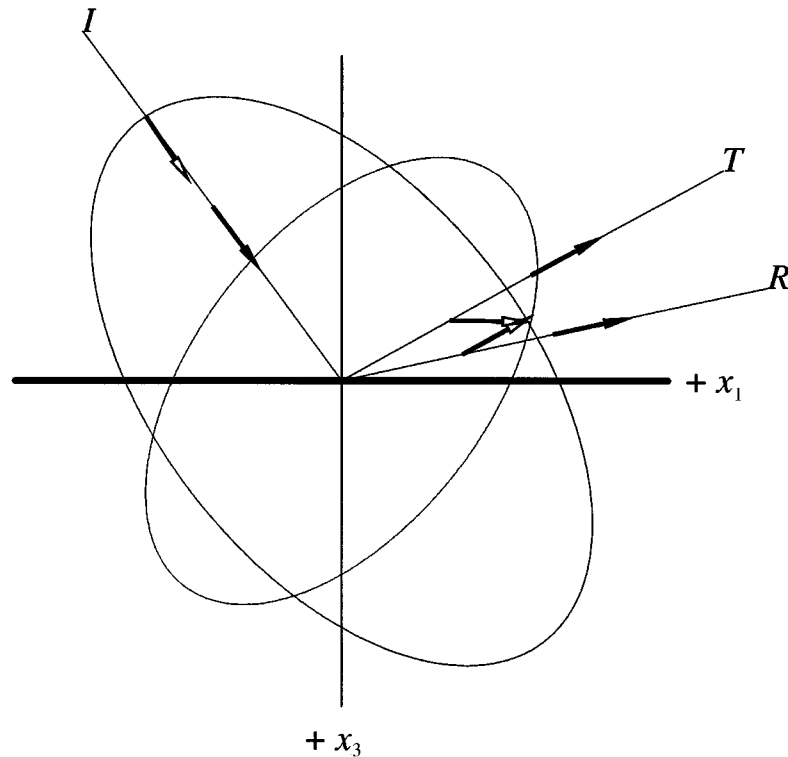
Figure 6. Directions of the real slowness and Umov–Poynting vectors, corresponding to the critical angle $\theta_C = 36.44°$ for the elastic case. At the critical angle and beyond, the refracted Umov–Poynting vector is parallel to the interface. Moreover, the refracted wave becomes evanescent.

mogeneous wave of the viscoelastic type ($\boldsymbol{\alpha}^\top \cdot \langle \boldsymbol{P} \rangle \neq 0$) in the refraction medium. However, this wave cannot propagate in an elastic medium (see equation (5.10)). ∎

A special case: Let us consider that both media are transversely isotropic and that $M_2 = M_1' = M_2' = M_1$. This case is very similar to the one studied by Krebes (1983) in isotropic media. Equation (6.8) gives the solution

$$\cot(\theta_C) = \frac{\rho c_{66}'}{\rho' c_{44}} - \frac{c_{66}}{c_{44}} \tag{6.13}$$

and $s_1 = \sqrt{\rho'/p_{66}'}$, which implies $s_3^T = 0$. The critical angle for this case is $\theta_C = 47.76°$. It can be shown from equations (4.2), (4.9), (4.10), (4.7) and (4.12) that the reflection and transmission coefficients are identical to those for perfect elasticity. However, beyond the critical angle, there is a normal interference flux (see §9 below) towards the boundary, complemented by a small energy flow away from the boundary in the transmission medium. This means that θ_C is a *discrete* critical angle, i.e. the Umov–Poynting vector of the refracted wave is parallel to the boundary only for the incident angle θ_C (in the elastic case this happens for $\theta^I \geqslant \theta_C$).

Since $s_3^T = 0$ at the critical angle, this occurs when the normal to the interface of abscissa $\mathrm{Re}(s_1)$ is tangent to the slowness curve of the refracted wave and, simultaneously, the normal to the interface with abscissa $\mathrm{Im}(s_1)$ is tangent to the attenuation

curve of the same wave. The analysis of this property for the general case will be given in a future paper.

7. Phase velocities and attenuations

The magnitude of the phase velocities can be obtained as the reciprocal of the slownesses. From equations (2.2) and (4.2), the phase velocity of the incident wave is simply

$$v_p^I = \{[\text{Re}(s_1)]^2 + [\text{Re}(s_3^I)]^2\}^{-1/2} = [\text{Re}(V^{-1})]^{-1}. \tag{7.1}$$

The phase velocity of the reflected wave is obtained from equation (4.5):

$$v_p^R = \{[\text{Re}(s_1)]^2 + [\text{Re}(s_3^R)]^2\}^{-1/2}, \tag{7.2}$$

or, using equations (2.10), (4.2) and (4.10),

$$v_p^R = \left\{(v_p^I)^{-2} + 4\sin(\theta^I)\,\text{Re}\left(p_{46}p_{44}^{-1}V^{-1}\right)\text{Re}(p_{44}^{-1}Z^I)\right\}^{-1/2}. \tag{7.3}$$

In the transversely isotropic case v_p^R equals v_p^I. In the elastic case, equation (7.3) reduces to

$$v_p^R = v_p^I\{1 + 4\sin(\theta^I)c_{46}c_{44}^{-1}[c_{46}c_{44}^{-1}\sin(\theta^I) + \cos(\theta^I)]\}^{-1/2}. \tag{7.4}$$

Moreover, when the incident Umov–Poynting vector is parallel to the interface, $Z^I = 0$, $s_3^I = s_3^R$ and $v_p^R = v_p^I$.

Similarly, the phase velocity of the refracted wave is obtained from equation (4.6):

$$v_p^T = \{[\text{Re}(s_1)]^2 + [\text{Re}(s_3^T)]^2\}^{-1/2}. \tag{7.5}$$

The phase velocities of the incident, reflected and refracted waves, versus the incidence angle, are represented in figure 7, where the dotted line corresponds to the elastic case. As can be seen, the elastic velocity is always higher than the viscoelastic velocity, since the elastic case is taken at the high-frequency limit.

When the incident Umov–Poynting vector is parallel to the interface, the phase velocity v_p^T is approximately equal to v_p^I, since, for our particular example, $c_{66}/c_{44} \approx c_{66}'/c_{44}'$ implies that $\text{Re}(s_3^T) \approx s_3^I$.

By virtue of equations (2.3), (4.2) and (4.5), the magnitudes of the incident and reflected attenuation vectors are given by

$$\alpha^I = \omega\{[\text{Im}(s_1)]^2 + [\text{Im}(s_3^I)]^2\}^{1/2} = -\omega\text{Im}(V^{-1}) \tag{7.6}$$

and

$$\alpha^R = \omega\{[\text{Im}(s_1)]^2 + [\text{Im}(s_3^R)]^2\}^{1/2} \tag{7.7}$$

or, using equations (2.10), (4.2) and (4.10),

$$\alpha^R = \left[(\alpha^I)^2 + 4\omega^2\sin(\theta)\text{Im}\left(p_{46}p_{44}^{-1}V^{-1}\right)\text{Im}(p_{44}^{-1}Z^I)\right]^{1/2}. \tag{7.8}$$

In the transversely isotropic case, $\alpha^R = \alpha^I$. Finally, the magnitude of the refracted attenuation vector is obtained from equation (4.6):

$$\alpha^T = \omega\{[\text{Im}(s_1)]^2 + [\text{Im}(s_3^T)]^2\}^{1/2}. \tag{7.9}$$

The attenuations are represented in figure 8. The high attenuation value of the refracted wave can be explained as follows. Figure 3 indicates that, at approximately
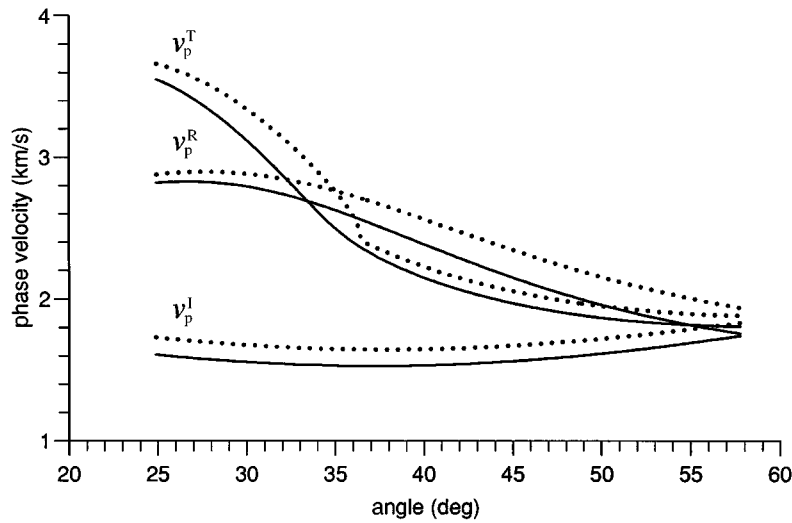
Figure 7. Phase velocities of the incident, reflected and refracted waves versus the incidence angle. The elastic case is represented by a dotted line.
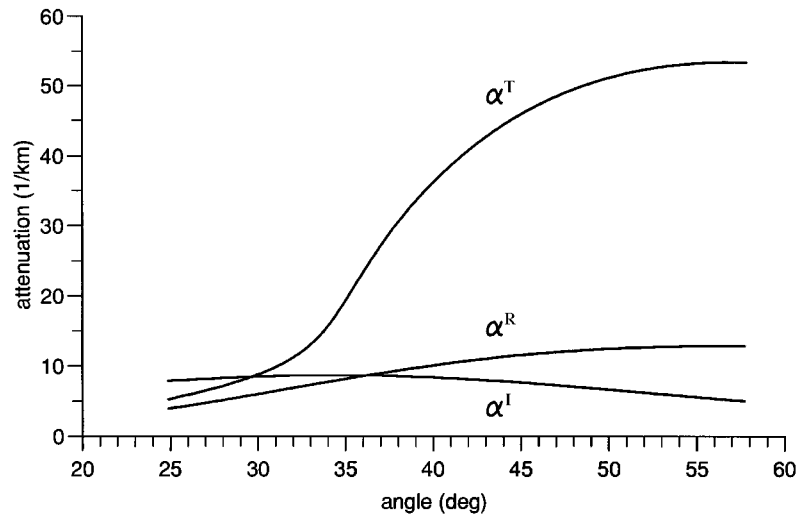
Figure 8. Attenuations of the incident, reflected and refracted waves versus the incidence angle.

the elastic critical angle and beyond, the energy angle of the refracted wave ψ^{T} is close to $\frac{1}{2}\pi$ and that the attenuation vector is almost perpendicular to the interface. In practice, this implies that the refracted wave behaves as an evanescent wave of the elastic type. This effect tends to disappear when the the intrinsic quality factors of the lower and/or upper media are lower than the values given in §3.

8. Energy flux balance

It is well known that to balance energy flux at an interface between two isotropic single-phase media, it is necessary to consider the *interaction* energy fluxes when the media are viscoelastic (Borcherdt 1977; Krebes 1983). In the incidence medium, for
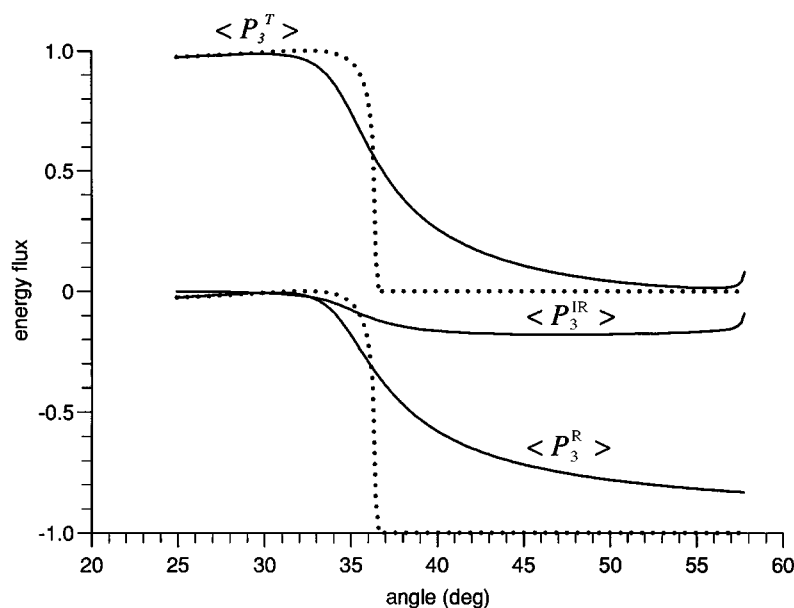
Figure 9. Normalized fluxes (energy coefficients) versus the incidence angle. The fluxes are normalized with respect to the incident flux. The elastic case is represented by a dotted line.

instance, they arise from the interaction of the stress and velocity fields of the incident and reflected waves. A similar phenomenon takes place at an interface separating two porous media when the fluid viscosity is different from zero. For instance, Dutta & Ode (1983) call them *interference* fluxes and show that they vanish for zero viscosity.

In a welded interface, the normal component of the average Umov–Poynting $\hat{\boldsymbol{e}}_3 \cdot \langle \boldsymbol{P} \rangle$ is continuous across the interface. This is a consequence of the boundary conditions that impose continuity of normal stress σ_{32} and particle velocity (Borcherdt 1977). Then, the balance of power flow at the interface can be expressed as

$$-\tfrac{1}{2}\operatorname{Re}[(\sigma_{32}^{\mathrm{I}} + \sigma_{32}^{\mathrm{R}})(v^{\mathrm{I}} + v^{\mathrm{R}})^*] = -\tfrac{1}{2}\operatorname{Re}(\sigma_{32}^{\mathrm{T}} v^{\mathrm{T}^*}). \tag{8.1}$$

Equation (8.1) is of the form

$$\langle P_3^{\mathrm{I}} \rangle + \langle P_3^{\mathrm{R}} \rangle + \langle P_3^{\mathrm{IR}} \rangle = \langle P_3^{\mathrm{T}} \rangle, \tag{8.2}$$

where

$$\langle P_3^{\mathrm{I}} \rangle = -\tfrac{1}{2}\operatorname{Re}(\sigma_{32}^{\mathrm{I}} v^{\mathrm{I}^*}) = \tfrac{1}{2}\omega^2 \operatorname{Re}(Z^{\mathrm{I}}) \exp[2\omega \operatorname{Im}(s_1)x_1] \tag{8.3}$$

is the incident flux,

$$\langle P_3^{\mathrm{R}} \rangle = -\tfrac{1}{2}\operatorname{Re}(\sigma_{32}^{\mathrm{R}} v^{\mathrm{R}^*}) = \tfrac{1}{2}\omega^2 |R|^2 \operatorname{Re}(Z^{\mathrm{R}}) \exp[2\omega \operatorname{Im}(s_1)x_1] \tag{8.4}$$

is the reflected flux,

$$\langle P_3^{\mathrm{IR}} \rangle = -\tfrac{1}{2}\operatorname{Re}(\sigma_{32}^{\mathrm{I}} v^{\mathrm{R}^*} + \sigma_{32}^{\mathrm{R}} v^{\mathrm{I}^*}) = \omega^2 \operatorname{Im}(R)\operatorname{Im}(Z^{\mathrm{I}}) \exp[2\omega \operatorname{Im}(s_1)x_1] \tag{8.5}$$

is the interference between the incident and reflected normal fluxes, and

$$\langle P_3^{\mathrm{T}} \rangle = -\tfrac{1}{2}\operatorname{Re}(\sigma_{32}^{\mathrm{T}} v^{\mathrm{T}^*}) = \tfrac{1}{2}\omega^2 |T|^2 \operatorname{Re}(Z^{\mathrm{T}}) \exp[2\omega \operatorname{Im}(s_1)x_1] \tag{8.6}$$

is the refracted flux. In the elastic case, Z^{I} is real and the interference flux vanishes.

The normalized normal fluxes (energy coefficients) versus the incidence angle are

shown in figures 9, with the dotted line representing the elastic case. Beyond the critical angle, the normal component of the refracted Umov–Poynting vector vanishes and there is no transmission to the lower medium. The energy travels along the interface and, as stated before, the plane wave is evanescent. In the viscoelastic case, these effects disappear and the reflected and refracted fluxes have to balance with a non-zero interference flux. Since the refracted flux is always greater than zero, there is transmission for all the incident angles.

9. Energy velocities and quality factors

The energy velocity $\boldsymbol{v}_e$ is the ratio of the average power flow density $\langle \boldsymbol{P} \rangle = \mathrm{Re}(\boldsymbol{P})$ to the mean energy density $\langle \epsilon_v + \epsilon_s \rangle$. For an incident homogeneous wave, substitution of (4.2) into (2.15) and use of (4.3) gives $\beta^{\mathrm{I}} = \rho V^2 / |V|^2$. Then, equations (2.13) and (2.16) imply

$$\langle \epsilon_v + \epsilon_s \rangle = \tfrac{1}{2} \rho \omega^2 \left(v_{\mathrm{p}}^{\mathrm{I}} \right)^{-1} \exp\{2\omega[\mathrm{Im}(s_1)x_1 + \mathrm{Im}(s_3^{\mathrm{I}})x_3]\} \ \mathrm{Re}(V), \qquad (9.1)$$

where v_{p} is the phase velocity. Finally, combining (2.9) and (9.1) gives

$$\boldsymbol{v}_e^{\mathrm{I}} = \frac{v_{\mathrm{p}}^{\mathrm{I}}}{\rho \, \mathrm{Re}(V)} \, \mathrm{Re}(X^{\mathrm{I}} \hat{\boldsymbol{e}}_1 + Z^{\mathrm{I}} \hat{\boldsymbol{e}}_3). \qquad (9.2)$$

The energy velocity of the reflected wave is obtained from equations (2.9), (2.13) and (2.16):

$$\boldsymbol{v}_e^{\mathrm{R}} = \frac{2 \, \mathrm{Re}(X^{\mathrm{R}} \hat{\boldsymbol{e}}_1 + Z^{\mathrm{R}} \hat{\boldsymbol{e}}_3)}{\rho + \mathrm{Re}(\beta^{\mathrm{R}})}, \qquad (9.3)$$

where $\beta^{\mathrm{R}} = \beta(s_3^{\mathrm{R}})$. If the upper medium has $p_{46} = 0$ (e.g. transverse isotropy), $Z^{\mathrm{R}} = -Z^{\mathrm{I}}$, $X^{\mathrm{R}} = X^{\mathrm{I}}$, $\beta^{\mathrm{R}} = \rho V^2 / |V|^2$, and after some algebra, it can be shown that $v_e^{\mathrm{R}} = v_e^{\mathrm{I}}$.

Similarly, the energy velocity of the refracted wave is

$$\boldsymbol{v}_e^{\mathrm{T}} = \frac{2 \, \mathrm{Re}(X^{\mathrm{T}} \hat{\boldsymbol{e}}_1 + Z^{\mathrm{T}} \hat{\boldsymbol{e}}_3)}{\rho' + \mathrm{Re}(\beta^{\mathrm{T}})}, \qquad (9.4)$$

where $\beta^{\mathrm{T}} = \beta(s_3^{\mathrm{T}})$.

An alternative expression for the energy velocity is obtained from the fact that, as in the elastic case, the phase velocity is the projection of the energy velocity onto the propagation direction. This relation was demonstrated by Carcione & Cavallini (1993) for inhomogeneous waves propagating in a general anisotropic viscoelastic medium. For antiplane plane shear waves we have that

$$v_e = v_{\mathrm{p}} / \cos(\psi - \theta). \qquad (9.5)$$

In terms of the tangents defined in §5,

$$v_e = v_{\mathrm{p}} \frac{\{[1 + \tan^2(\psi)][1 + \tan^2(\theta)]\}^{1/2}}{[1 + \tan(\psi)\tan(\theta)]}. \qquad (9.6)$$

The energy velocities of the incident, reflected and refracted waves, versus the incidence angle, are represented in figures 10, with the dotted line corresponding to the elastic case. Comparison of figures 7 and 10 indicates that the energy velocity in anisotropic viscoelastic media is greater or equal than the phase velocity (as predicted by equation (9.5)).
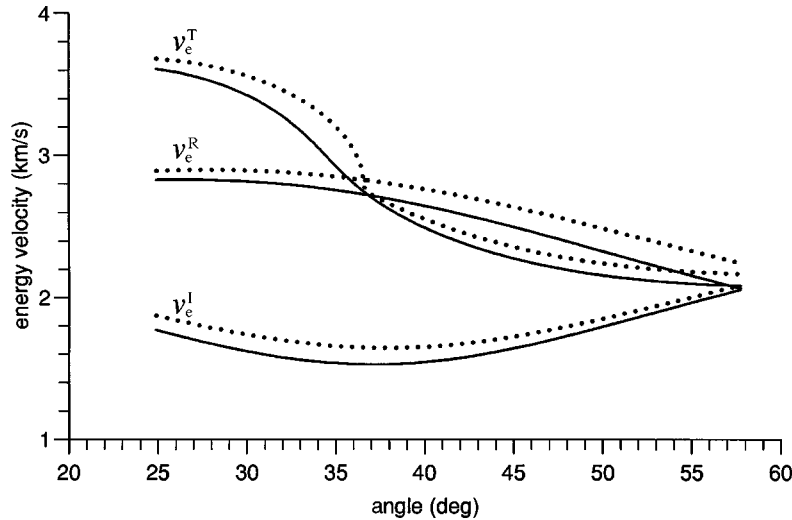
Figure 10. Energy velocities of the incident, reflected and refracted waves versus the incidence angle. The elastic case is represented by a dotted line.

The quality factor is the ratio of twice the average strain energy density (2.13) to the dissipated energy density (2.16). For the incident homogeneous wave it is simply

$$Q^{\mathrm{I}} = \frac{\mathrm{Re}(V^2)}{\mathrm{Im}(V^2)}. \tag{9.7}$$

while for the reflected and refracted waves,

$$Q^{\mathrm{R}} = \frac{\mathrm{Re}(\beta^{\mathrm{R}})}{\mathrm{Im}(\beta^{\mathrm{R}})} \tag{9.8}$$

and

$$Q^{\mathrm{T}} = \frac{\mathrm{Re}(\beta^{\mathrm{T}})}{\mathrm{Im}(\beta^{\mathrm{T}})}, \tag{9.9}$$

respectively. When $p_{46} = 0$, $\beta^{\mathrm{R}} = \rho V^2/|V|^2$, and $Q^{\mathrm{R}} = Q^{\mathrm{I}}$.

Let us consider the incident homogeneous wave. From equation (4.3), $\rho V^2 = p_{44}$ along the x_3-axis. Substitution of (3.1) into (9.7) and use of (3.2) gives equation (3.5). Then, the quality factor along the vertical direction is Q_{01} at the reference frequency f_0. Similarly, it can be shown that Q_{02} is the quality factor along the horizontal direction.

The quality factors are represented in figure 11. Like the attenuations (figure 8), the quality factors of the reflected and transmitted waves show a substantial anisotropic behaviour.

In a recent paper, Carcione & Cavallini (1995c) have demonstrated that the equations describing propagation of the TM (transverse magnetic) mode in a conducting anisotropic medium are completely analogous, from the mathematical point of view, to the propagation of viscoelastic antiplane shear waves in the plane of symmetry of a monoclinic medium. The equivalence identifies the magnetic field with the particle velocity, the electric field with the stress components, and the compliance components p_{IJ}^{-1} with the complex dielectric components. Therefore, the present
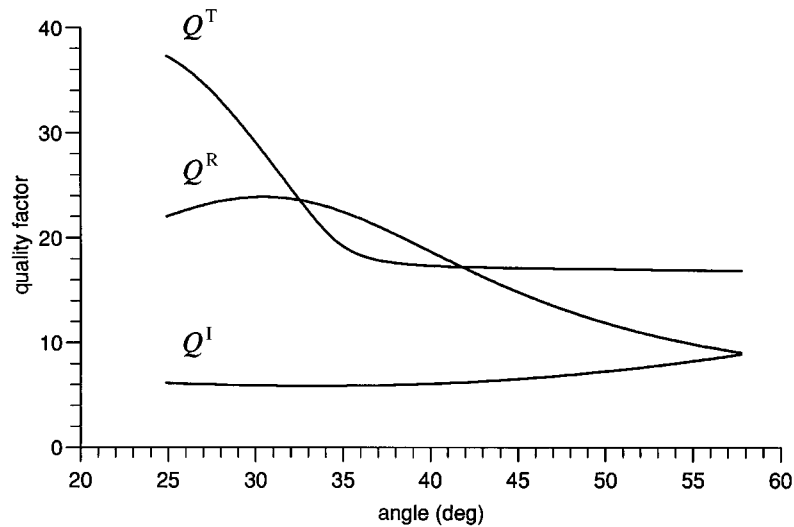
Figure 11. Quality factors of the incident, reflected and refracted waves versus the incidence angle.

reflection–refraction analysis can be applied to the electromagnetic case with minor modifications.

As in the homogeneous case (Carcione *et al.* 1996), confrontation of the present theory with numerical simulations may confirm some of the results and provide further insights into the physics of the problem. Additional work should consider an incident inhomogeneous plane wave and an analysis of the reflection–refraction problem including quasi-compressional and quasi-shear propagation modes.

10. Conclusions

Reflection and refraction in anisotropic–viscoelastic media present substantial differences compared to isotropic–elastic media. First, the multiple configurations, arising from different orientations of the principal axes with respect to the interface plane, imply different physical situations. The numerical example considered here intends to provide a comprehensive description of the different phenomena. Second, Snell's law in viscoelastic media considers also the attenuation vector, that plays the same role as the propagation vector. The presence of anisotropy implies that the relevant phenomena, as critical refraction, are related to the energy direction rather than the propagation direction. On the other hand, attenuation severely restricts the existence of critical and Brewster angles, and requires the existence of an interference flux between the incident and refracted waves, to balance energy flow.

This study considers a fixed frequency and an incident homogeneous wave. Therefore, additional research is necessary to study the effects of frequency and inhomogeneity of the incident wave on the reflection and refraction coefficients. Moreover, confrontation of the theory with numerical simulations may provide further insight into the physics of the problem.

The present reflection–refraction analysis can be applied to the TM electromagnetic case with minor modifications.

References

Auld, B. A. 1990 *Acoustic fields and waves in solids* (ed. R. E. Krieger), 2nd edn, vol. 2. Florida: Malabar.

Ben-Menahem, A. B. & Singh, S. J. 1981 *Seismic waves and sources*. New York: Springer.

Borcherdt, R. D. 1977 Reflection and refraction of type-II S waves in elastic and anelastic media. *Bull. Seism. Soc. Am.* **67**, 43–67.

Born, M. & Wolf, E. 1964 *Principles of optics*. Oxford: Pergamon.

Brekhovskikh, L. M. 1960 *Waves in layered media*. New York: Academic.

Buchen, P. W. 1971 Reflection, transmission and diffraction of SH-waves in linear viscoelastic solids. *Geophys. Jl R. Astr. Soc.* **25**, 97–113.

Carcione, J. M. 1994 Wavefronts in dissipative anisotropic media. *Geophysics* **59**, 644–657.

Carcione, J. M. & Cavallini, F. 1993 Energy balance and fundamental relations in anisotropic-viscoelastic media. *Wave motion* **18**, 11–20.

Carcione, J. M. & Cavallini, F. 1994 A semi-analytical solution for the propagation of pure shear waves in dissipative monoclinic media. *Acoustics Letters* **17**, 72–76.

Carcione, J. M. & Cavallini, F. 1995*a* Forbidden directions for inhomogeneous pure shear waves in dissipative anisotropic media. *Geophysics* **60**, 522–530.

Carcione, J. M. & Cavallini, F. 1995*b* The generalized SH-wave equation. *Geophysics* **60**, 549–555.

Carcione, J. M. & Cavallini, F. 1995*c* On the acoustic-electromagnetic analogy. *Wave motion* **21**, 149–162.

Carcione, J. M., Quiroga-Goode, G. & Cavallini, F. 1996 Wavefronts in dissipative anisotropic media: comparison of the plane wave theory with numerical modeling. *Geophys.* **61**, 857–861.

Caviglia, G. & Morro, A. 1992 *Inhomogeneous waves in solids and fluids*. Singapore: World Scientific.

Dutta, N. C. & Ode, H. 1983 Seismic reflections from a gas–water contact. *Geophysics* **48**, 14–32.

Hayes, M. A. & Rivlin, R. S. 1974 Plane waves in linear viscoelastic materials. *Q. Appl. Math.* **32**, 113–121.

Henneke II, E. G. 1971 Reflection-refraction of a stress wave at a plane boundary between anisotropic media. *J. Acoust. Soc. Am.* **51**, 210–217.

Helbig, K. 1994 *Foundations of anisotropy for exploration seismics*. Oxford: Pergamon.

Horgan, C. O. 1995 Antiplane shear deformations in linear and nonlinear solid mechanics. *SIAM Rev.* **37**, 53–81.

Johnston, D. H. 1987 Physical properties of shale at temperature and pressure. *Geophysics* **52**, 1391–1401.

Krebes, E. S. 1983 The viscoelastic reflection/transmission problem: two special cases. *Bull. Seism. Soc. Am.* **73**, 1673–1683.

Krebes, E. S. 1984 On the reflection and transmission of viscoelastic waves—some numerical results. *Geophysics* **49**, 1374–1380.

Krebes, E. S. & Le, L. H. T. 1994 Inhomogeneous plane waves and cylindrical waves in anisotropic anelastic media. *J. Geophys. Res.* **99**, 23 899–23 919.

Le, L. H. T. 1993 On Cagniard's problem for a qSH line source in transversely-isotropic media. *Bull. Seism. Soc. Am.* **83**, 529–541

Le, L. H. T., Krebes, E. S. & Quiroga-Goode, G. E. 1994 Synthetic seismograms for SH waves in anelastic transversely isotropic media. *Geophys. Jl Int.* **116**, 598–604.

Musgrave, M. J. P. 1970 *Crystal acoustics*. San Francisco, CA: Holden-Day.

Oughstun, K. E. & Sherman, G. C. 1994 *Electromagnetic pulse propagation in causal dielectrics*. Berlin: Springer.

Rokhlin, S. I., Bolland, T. K. & Adler, L. 1986 Reflection–refraction of elastic waves on a plane interface between two generally anisotropic media. *J. Acoust. Soc. Am.* **79**, 906–918.

Romeo, M. 1994 Inhomogeneous waves in anisotropic dissipative solids. *Q. Jl. Mech. Appl. Math.* **47**, 482–491.

Schoenberg, M. 1971 Transmission and reflection of plane waves at an elastic-viscoelastic interface, *Geophys Jl R. Astr. Soc.* **25**, 35–47.

Schoenberg, M. & Costa, J. 1991 The insensitivity of reflected SH waves to anisotropy in an underlying layered medium. *Geophys. Prosp.* **39**, 985–1003.

Zener, C. 1948 *Elasticity and anelasticity of metals.* University of Chicago Press.